Delft University of Technology

Document Version
Final published version

Citation (APA)
Paul, A., & Pereira, S. F. (2025). Implementation of quad detection scheme in coherent Fourier scatterometry for inspection of patterned structures. In P. Lehmann, W. Osten, & A. A. Goncalves (Eds.), *Optical Measurement Systems for Industrial Inspection XIV* Article 135671I (Proceedings of SPIE - The International Society for Optical Engineering; Vol. 13567). SPIE. https://doi.org/10.1117/12.3062040

Important note
To cite this publication, please use the final published version (if applicable).
Please check the document version above.

Copyright
In case the licence states "Dutch Copyright Act (Article 25fa)", this publication was made available Green Open Access via the TU Delft Institutional Repository pursuant to Dutch Copyright Act (Article 25fa, the Taverne amendment). This provision does not affect copyright ownership.
Unless copyright is transferred by contract or statute, it remains with the copyright holder.

Sharing and reuse
Other than for strictly personal use, it is not permitted to download, forward or distribute the text or part of it, without the consent of the author(s) and/or copyright holder(s), unless the work is under an open content license such as Creative Commons.

Takedown policy
Please contact us and provide details if you believe this document breaches copyrights.
We will remove access to the work immediately and investigate your claim.

This work is downloaded from Delft University of Technology.

Green Open Access added to TU Delft Institutional Repository
as part of the Taverne amendment.

More information about this copyright law amendment
can be found at https://www.openaccess.nl.

Otherwise as indicated in the copyright section:
the publisher is the copyright holder of this work and the
author uses the Dutch legislation to make this work public.

Implementation of quad detection scheme in coherent Fourier scatterometry for inspection of patterned structures

Anubhav Paul* and Silvania F. Pereira

Imaging Physics Department, Faculty of Applied Sciences, Delft University of Technology, Lorentzweg 1, 2628 CJ Delft, The Netherlands

ABSTRACT

Coherent Fourier scatterometry (CFS) is a powerful scanning technique for inspecting defects on structured surfaces, relying on split detectors to measure asymmetry in the far-field scattered light. The split signal, a differential signal derived by subtracting signals from opposing halves of the detector, effectively detects asymmetries along the scan direction. However, this approach is inherently limited when inspecting patterned structures, as it loses information orthogonal to the scan direction. This results in signals that vary depending on the orientation of the patterns, complicating the characterization of certain defects. To overcome this limitation, we introduce a quad detector-based CFS scheme. By utilizing four independent photodetectors and processing their signals to generate integrated, split, and quad outputs, we capture complete far-field information. A Fourier filtering step removes detector-specific offsets, enabling robust signal analysis. Unlike the split-detector approach, this method provides defect and nanostructure inspection independent of the shape and orientation of the underlying patterns. We present the results of implementing this scheme to inspect defects on patterned surfaces. The quad detector signal reveals the edges of defects and demonstrates the versatility of this approach across different surface features. This advancement enhances the capability of CFS for defect inspection, offering a comprehensive and reliable solution for patterned structures where traditional split-detector methods fall short.

Keywords: coherent Fourier scatterometry, quad detector, inspection, nanostructures

1. INTRODUCTION

The demand for precise and reliable inspection of patterned nanostructures is rapidly growing as semiconductor devices continue to scale down in size. Advanced manufacturing nodes, often involving complex three-dimensional architectures and heterogeneous materials, present a host of metrological challenges.[1,2] Accurate characterization and detection of defects within such structures are pivotal for ensuring device functionality, yield, and manufacturability. The challenges are amplified by the arbitrary orientation of structural features and by the fact that many critical defects manifest at the edges of these patterns, which may be buried or obscured by the surrounding geometry.

Traditional inspection techniques such as scanning electron microscopy (SEM)[3] and atomic force microscopy (AFM)[4] offer nanometric resolution but are inherently limited by low throughput, invasiveness, and incompatibility with in-line inspection requirements. Brightfield optical inspection techniques have also been used for feature detection.[5,6] However, their effectiveness diminishes at sub-wavelength scales due to the inherent constraint by Abbe's diffraction limit, further, they have strong dependence on the illumination angle, polarization, and defect orientation. Moreover, they require extensive calibration or precise optical setup, and their defect sensitivity can vary significantly across different patterned structures with different geometries or orientations.

Coherent Fourier scatterometry (CFS) has emerged as a promising optical technique capable of non-invasive, inline inspection/detection and characterization of nanoparticles with subwavelength sensitivity.[7–9] Traditional implementations of CFS utilize a split detector to measure the differential signal along the scanning direction. While this configuration is highly sensitive to asymmetries along that axis, it inherently loses information orthogonal to the scan direction. This trade-off limits its applicability to arbitrarily oriented patterns and complex surfaces, such as gratings or photonic crystals, where edge detection is critical.[10]

*Contact author: A.Paul-1@tudelft.nl

Optical Measurement Systems for Industrial Inspection XIV, edited by Peter Lehmann,
Wolfgang Osten, Armando Albertazzi Gonçalves, Proc. of SPIE Vol. 13567, 135671I
2025 Published by SPIE · 0277-786X · doi: 10.1117/12.3062040

To address this limitation, we present the implementation of a quad detector-based CFS scheme. This detector configuration utilizes four independent photodetectors arranged in a quadrant geometry, allowing the extraction of multiple signal outputs, including integrated intensity, left-right (LR) and top-bottom (TB) split signals, and a novel quad signal. The quad signal, in particular, enables sensitivity to edges in all directions, independent of their orientation on the wafer surface. This advancement significantly enhances the defect detection capabilities of CFS for complex, patterned nanostructures.

In this paper, we describe the implementation of the quad detection scheme in CFS and the data processing pipeline. We further present experimental results demonstrating the detection of 150 nm PSL nanoparticles and patterned nanostructures. For nanoparticles, we demonstrate the capability of the quad signal to reveal edge features and analyze the influence of the system's point spread function (PSF) on the observed signal morphology, showing how polarization-dependent beam affects the edge response. For patterned structures, we show that the quad signal successfully captures edge information across all orientations, overcoming the inherent directional limitations of traditional split detection and enabling comprehensive inspection of arbitrarily oriented features.

2. METHODS

2.1 Implementation of Quad Detection Scheme

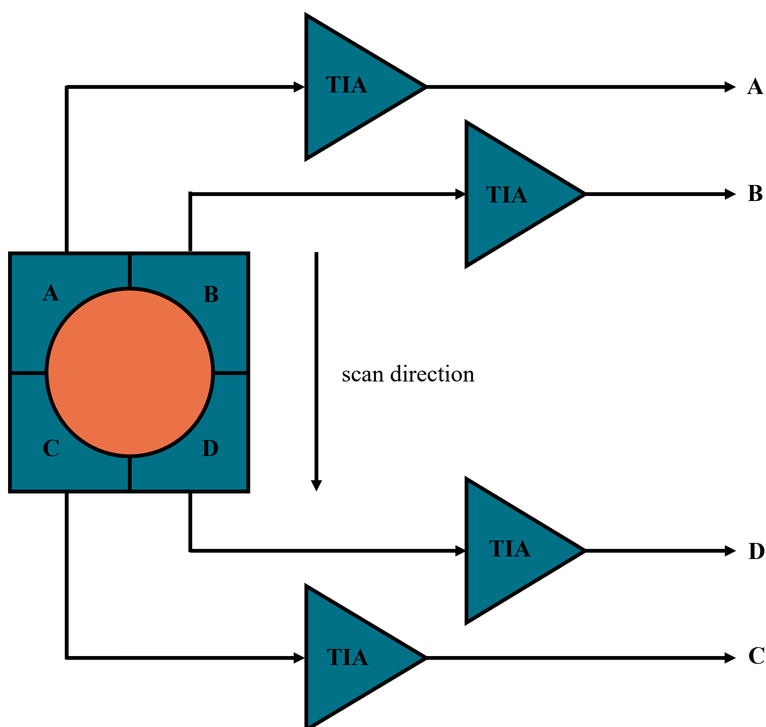

Figure 1: Schematic of the quad detector.

In CFS, the far-field scattering pattern carries crucial spatial information about surface morphology and defects. The detection system acts not merely as a passive receiver but as a mathematical operator, transforming this spatial distribution into a measurable signal that emphasizes certain features over others. Traditional implementations of CFS rely on a split detector, which computes the differential signal between opposing halves of the scattered field. Mathematically, this corresponds to applying a first-order directional gradient, analogous to edge detection filters used in image processing, such as the Prewitt operator.

To overcome the directional limitation of split detection, we introduce a quad detector-based scheme. This configuration comprises four independent photodetector elements, denoted A, B, C, and D, arranged in a quadrant geometry (see Fig. 1). Each photodetector outputs a current signal, which is converted into a voltage using a

dedicated transimpedance amplifier (TIA). The TIA provides high sensitivity and linear conversion, enabling precise capture of optical power fluctuations across the four quadrants. The quad detector is carefully aligned such that the incident beam is centered at the intersection of the four pixels, maximizing symmetry and ensuring balanced baseline response.

From these four voltage signals, we compute several derived outputs that encode different spatial characteristics of the scattered field:

$$\text{I signal} = A + B + C + D, \tag{1a}$$

$$\text{SD}_{\text{LR}} \text{ signal} = (A + B) - (C + D), \tag{1b}$$

$$\text{SD}_{\text{TB}} \text{ signal} = (A + C) - (B + D), \tag{1c}$$

$$\text{QD signal} = \sqrt{2[(A - D)^2 + (B - C)^2]}. \tag{1d}$$

These operators can be interpreted as spatial filters: the SD_{LR} and SD_{TB} correspond to directional derivatives along orthogonal axes (akin to Prewitt masks), while the QD signal approximates the Euclidean norm of the gradient, providing isotropic edge sensitivity.

2.1.1 Data processing

Accurate edge detection in CFS requires minimizing detector-specific noise and offset. Due to slight misalignments, the beam may not be centered perfectly on the quad detector, leading to distinct DC offsets in the individual channels. To address this, we employ Fourier filtering to suppress the central DC component of each detector signal prior to calculating the derived outputs. This process ensures uniform baseline correction and enhances signal contrast.

After DC offset removal, the signals are processed pixel-by-pixel using Eqs. 1(a)-(d) to generate spatial maps for integrated, split, and quad outputs. These outputs can be interpreted as different modalities of the same optical measurement, each highlighting a distinct feature class: intensity (I), direction-specific asymmetry (SD), and orientation-independent edges (QD).

2.2 Experimental Setup

The experimental realization of the CFS system with quad detection is shown schematically in Fig. 2. A 633 nm He-Ne laser provides a coherent, collimated beam that serves as the illumination source. The beam passes through a rotatable polarizer (P), allowing control over the direction of the incident linear polarization illumination. In this study, we use an arbitrary polarization direction for the measurements. The beam is directed onto the sample using a non-polarizing beam splitter (BS) and a high numerical aperture (NA=0.9) objective lens (O), which tightly focuses the beam onto the sample (S). The sample is mounted on a piezo-controlled XYZ translation stage (XYZ TS) and scanned in a serpentine pattern to acquire spatially resolved measurements over the target area. The scattered light from the sample is collected in reflection mode, passing back through the objective and redirected by the BS into the detection path. A 4f (L1 and L2) relay lens system images the back focal plane (BFP) of the objective onto the detection plane, where the quad detector is positioned. The quad detector is mounted on a holder equipped with two orthogonal alignment screws. These allow fine adjustment of the detector position to ensure precise centering of the focused beam on the detector quadrants. Accurate alignment is critical for minimizing signal imbalance and ensuring the correct computation of integrated, split, and quad signals as described in Section 2.1.

3. RESULTS

3.1 Inspection of Nanoparticles

To evaluate the performance of the quad detection scheme, we first scanned a 25×25 μm area of a sample containing 150 nm polystyrene latex (PSL) nanoparticles on Si wafer. Figure 3 shows the raw voltage signals obtained from the four photodetector channels (A, B, C, and D), after removal of the DC background using

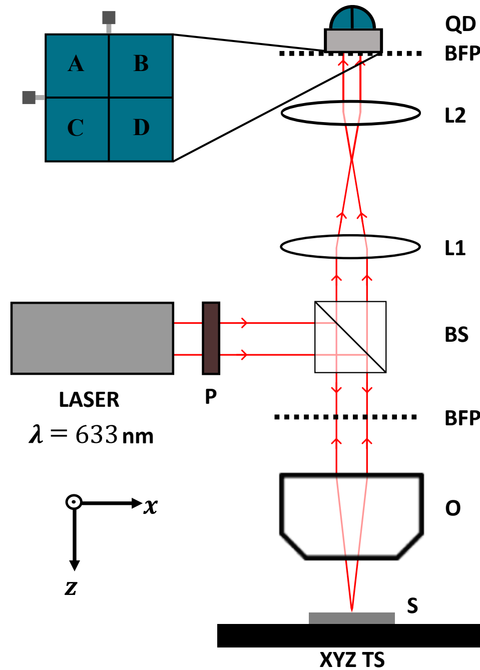

Figure 2: Schematic of the experimental setup of coherent Fourier scatterometry (CFS).

Fourier filtering. These signals form the basis for all subsequent outputs. Here, the individual channel signals show weak signals arising from the scattering of the PSL nanoparticles.

In Fig. 4 we show the 25×25 μm CFS scanned maps of I, $\mathrm{SD_{LR}}$, $\mathrm{SD_{LR}}$, and QD signal of 150 nm PSL nanoparticles. These signals were computed using Eq. 2 on the individual photodetector channel signals A, B, C, and D. The I signal shows the total intensity of the scattered field. While this mode captures the presence of particles through intensity variation, it lacks directional sensitivity and edge specificity. The SD signals (SD_{LR} and SD_{TB}) highlight asymmetries in the far-field scattering pattern, producing characteristic dipole-like lobes aligned with the scan direction. This result mirrors previous implementations of CFS using single-axis split detectors and is effective for detecting directional features or off-center scattering profiles. However, as shown in Fig. 4, the QD signal provides a fundamentally different representation. It reveals ring-like patterns corresponding to the edges of the particles, with much clearer definition and isotropic contrast. This demonstrates that the QD signal is sensitive to gradients and edges irrespective of their orientation relative to the scan axis.

Interestingly, as shown in Fig. 5, the rings observed around the particles are not perfectly circular, but rather elliptical. This shape distortion is linked to the ellipticity of the point spread function (PSF) of the system, caused by the high numerical aperture (NA) of the illumination beam. To verify this, we performed measurements with different polarization orientations of the incident beam. Figure 5 shows the QD signal for two different arbitrary incident illumination polarization directions defined by angle $\theta \sim 20°$ (left) and $\theta \sim 90°$ (right). Notably, the orientation of the elliptical edge response rotates with the polarization, confirming that the observed ellipticity is not intrinsic to the particles but originates from the illumination PSF. Insets in Fig. 5 show a zoom into a single particle and measure the edge dimensions of the PSF (L1~ 0.9 μm, L2~ 0.7 μm), clearly illustrating that the quad signal is tracking the PSF footprint rather than the physical size of the particle. This highlights that for subspot-size particles, the edge detection reflects the intensity gradient of the beam rather than the actual object boundary. As the particle size approaches the illumination spot size, the quad signal is expected to more accurately trace the physical edges.

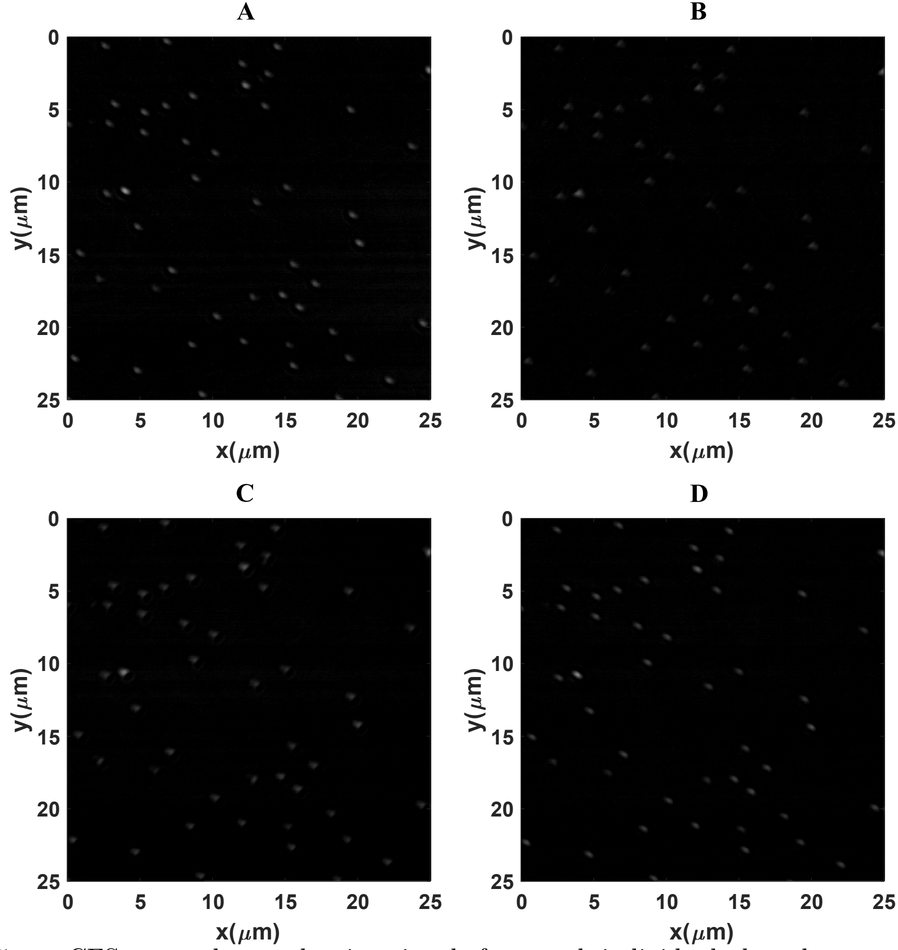

Figure 3: 25×25 μm CFS scanned map showing signals from each individual photodetector (A, B, C, and D) of 150 nm PSL nanosparticles on Si wafer.

3.1.1 SNR

The signal-to-noise ratio (SNR) for the different outputs can be compared by computing the power ratio between signal and background regions. For the quad signal, we define it as:

$$\mathrm{SNR}_{\mathrm{dB}}^{\mathrm{QD}} = 10\log_{10}\frac{P_{sig}^{\mathrm{QD}}}{P_{noise}^{\mathrm{QD}}} = 10\log_{10}\frac{P_{sig}^{\mathrm{SD_{LR}}} + P_{sig}^{\mathrm{SD_{TB}}}}{P_{noise}^{\mathrm{SD_{LR}}} + P_{noise}^{\mathrm{SD_{TB}}}}, \tag{2}$$

where, P_{sig}^{QD}, $P_{sig}^{\mathrm{SD_{LR}}}$, and $P_{sig}^{\mathrm{SD_{TB}}}$ is the power of the signal (contained at the edges of the nanostructure) for QD, $\mathrm{SD_{LR}}$, and $\mathrm{SD_{TB}}$ signals, respectively, and P_{noise}^{QD}, $P_{noise}^{\mathrm{SD_{LR}}}$, and $P_{noise}^{\mathrm{SD_{TB}}}$ is the background noise of the QD, $\mathrm{SD_{LR}}$, and $\mathrm{SD_{TB}}$ signals, respectively. According to Eq. 2, the $\mathrm{SNR}_{\mathrm{dB}}^{\mathrm{QD}} = 10.76$ for the 150 nm PSL nanoparticles. We similarly calculate, $\mathrm{SNR}_{\mathrm{dB}}^{\mathrm{SD_{LR}}} = 9.93$ and $\mathrm{SNR}_{\mathrm{dB}}^{\mathrm{SD_{TB}}} = 11.26$. The QD signal does not necessarily yield the highest SNR. In practice, one of the individual split signals may achieve better contrast or exhibit lower background noise, resulting in superior SNR compared to the combined QD output. This indicates that the QD signal offers a balance between noise suppression and feature completeness, rather than maximizing SNR alone. However, the key advantage of the QD signal lies in its orientation-invariant edge detection, which makes it particularly effective for irregularly oriented nanostructure patterns or situations where split detection may fail to provide consistent output.

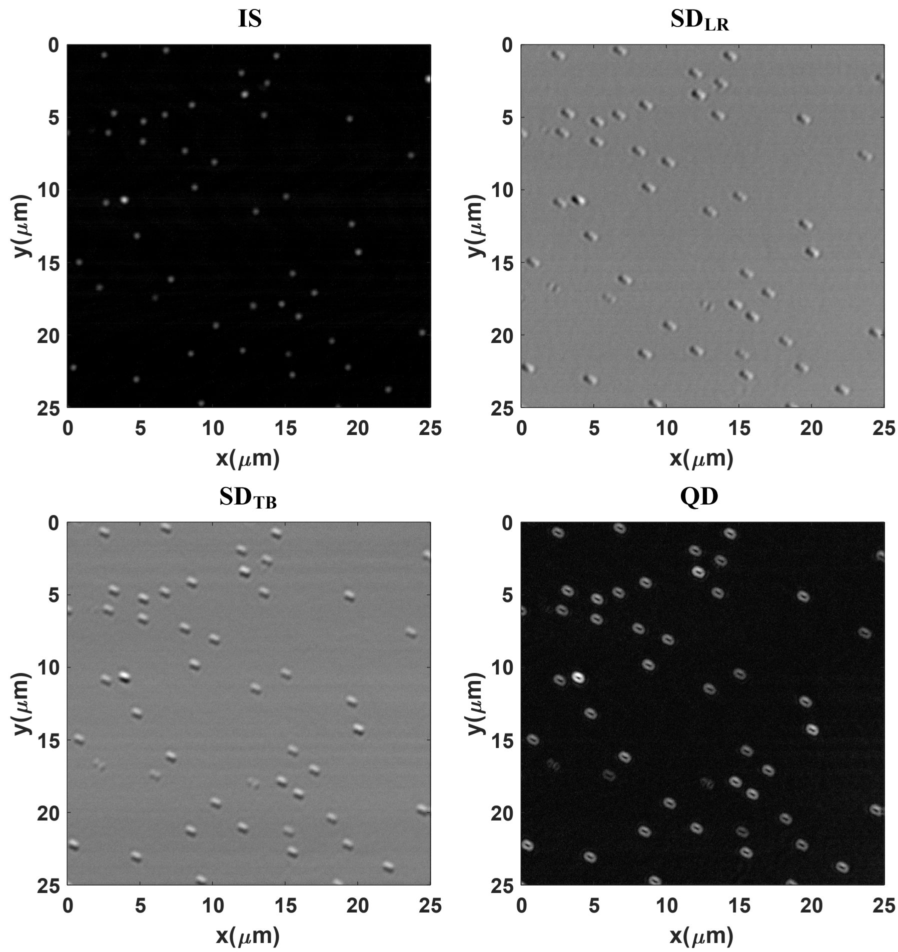

Figure 4: 25×25 μm CFS scanned map showing I, SD_{LR}, SD_{LR}, and QD signal of 150 nm PSL nanosparticles on Si wafer (obtained using Eq. 1).

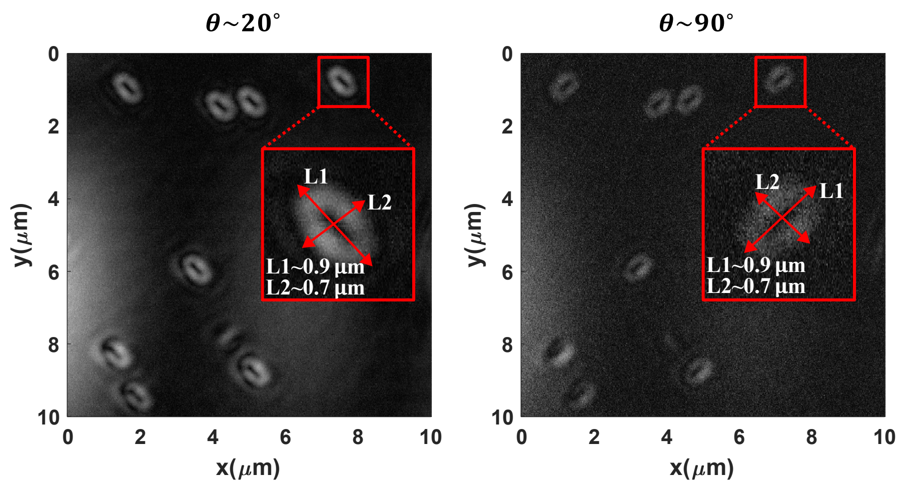

Figure 5: 10×10 μm CFS scanned map showing QD signal of 150 nm PSL nanosparticles for two different illumination polarization directions defined by angle $\theta \sim 20°$ (left) and $\theta \sim 90°$ (right).

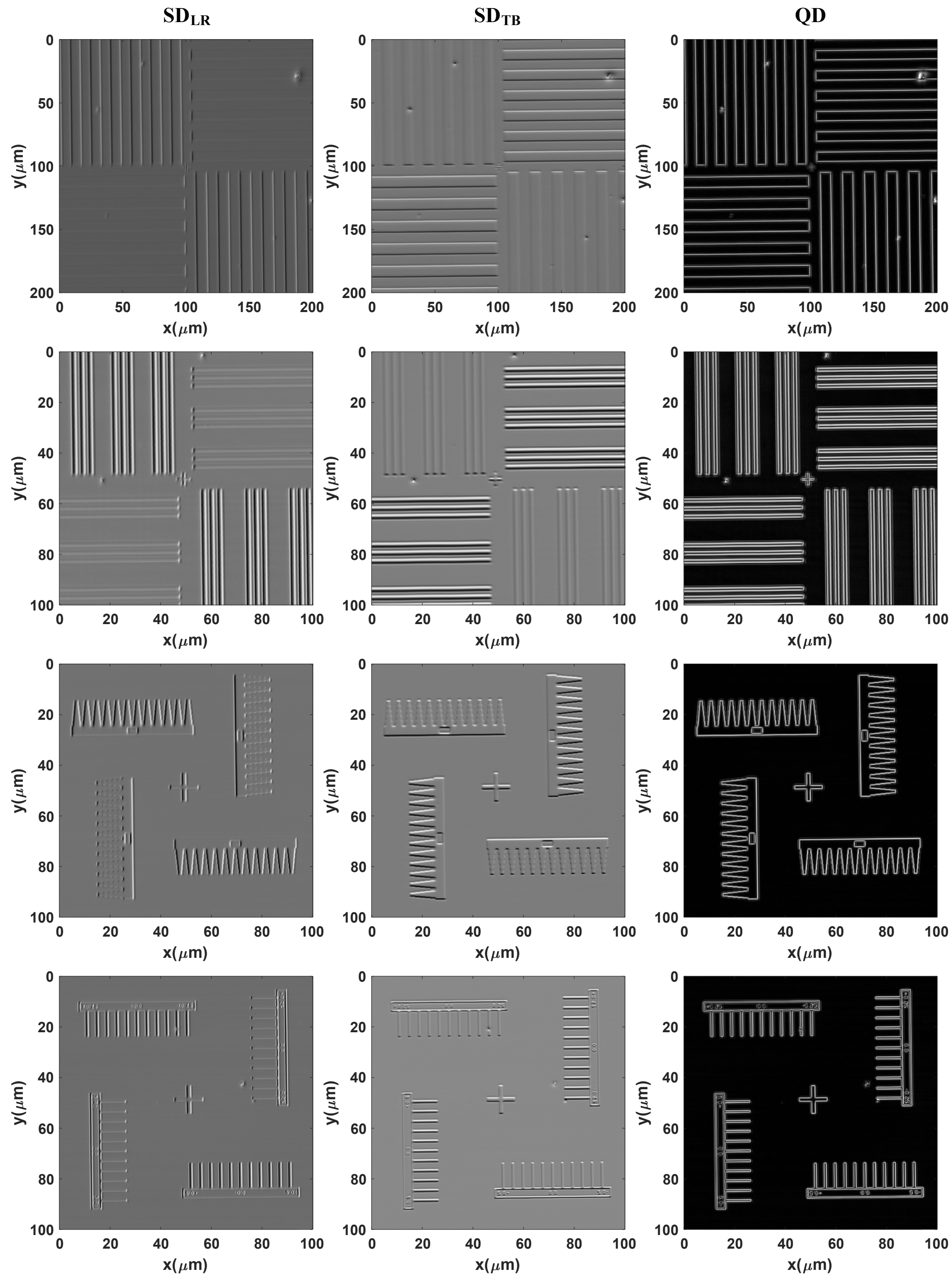

Figure 6: CFS scans of four different types of markers fabricated on Si wafer. (left column) showing SD_{LR} signal; (middle column) showing SD_{TB} signal; (right column) showing QD signal. Here we can also detect the defects on top of the nanostructures.

3.2 Inspection of Patterned Nanostructures

Having validated the scheme on symmetric particles, we turn to its primary application: inspecting patterned nanostructures with arbitrary feature orientation. Figure 6 presents the SD_{LR} (left column), SD_{TB} (middle column), and QD (right column) obtained from various marker patterns, such as crossed lines (two patterns), and saw tooth patterns (two patterns), fabricated on a wafer. These features span a range of orientations and edge profiles. The split signals in this case exhibit strong directional bias; edges aligned with the gradient axis are highlighted, while orthogonal features are suppressed or distorted. As a result, fine details, such as corner shapes, edge defects, or small indentations, are either missed or partially resolved in the SD maps. In contrast, the quad signal in Fig. 6 provides a uniform edge representation, capturing all edge orientations simultaneously. This confirms the central premise of the quad detection scheme, which enables orientation-independent edge detection, crucial for inspecting nanostructures, which may not be aligned with the scan direction.

In summary, the quad detector scheme significantly expands the applicability of CFS. It enhances edge contrast, maintains rotational invariance, and enables more robust defect detection for complex surface features.

4. DISCUSSIONS AND CONCLUSIONS

The results presented in this work demonstrate the significant advantages of incorporating a quad detection scheme into coherent Fourier scatterometry (CFS) for the inspection of patterned surfaces and nanostructures. Traditional split detection approaches, while highly sensitive to directional asymmetries, are inherently limited by their one-dimensional nature. This becomes particularly problematic when inspecting patterned features with arbitrary orientations or complex geometries, where directional information is insufficient to resolve edge locations uniformly.

The quad detector overcomes this limitation by combining four quadrant signals to compute outputs that are sensitive to intensity gradients in multiple directions. The derived quad signal (QD) acts effectively as a rotationally invariant edge operator, capturing feature boundaries regardless of their alignment. This isotropic sensitivity was validated through measurements on both spherical nanoparticles and patterned nanostructures. In the case of PSL particles, the quad signal revealed ring-like edge responses, providing a clear visualization of particle presence even when their size is smaller than the illumination spot. The observed ellipticity in the ring shapes was directly linked to the asymmetry of the point spread function (PSF), which is elongated along the polarization direction of the beam at the objective, highlighting the sensitivity of the quad signal to both the sample and the illumination system.

The signal-to-noise ratio (SNR) analysis further clarifies the strengths and trade-offs of the quad detection approach. Although QD output does not outperform individual split signals in terms of SNR, especially when one directional component dominates, the combination of channels provides a more robust and complete representation of edge information. Importantly, the SNR of the quad signal remains comparable to that of the best-performing split channel, suggesting that added directional coverage does not come at a significant cost in sensitivity.

The inspection of patterned nanostructures highlights the strength of the quad detection scheme, its ability to consistently detect edges across a wide range of orientations. Where split detectors fail to register features orthogonal to their gradient direction, the quad detector successfully resolves these structures, enabling comprehensive inspection. This capability is particularly relevant as semiconductor architectures become increasingly non-uniform, with critical features that are not aligned with the scan axis or have complex curvatures.

In conclusion, the implementation of a quad detector in a CFS framework addresses a critical limitation of conventional split detection methods by enabling full-directional edge sensitivity. The method provides multiple output modalities—integrated, split, and quad signals—that can be flexibly utilized depending on the inspection task. The approach is compatible with existing CFS setups and only requires changes to the detection and signal processing pipeline. Future work will explore the extension of this scheme to higher-dimensional detector arrays and the use of custom kernel combinations to extract more advanced morphological information from the far-field signal.

ACKNOWLEDGMENTS

We acknowledge the Nederlandse Organisatie voor Wetenschappelijk Onderzoek (Project 17-24 Synoptics No. 2) for funding this research. We would like to thank Roland Horsten of TU Delft for designing and producing the quad detector.

REFERENCES

[1] Mansfield, E., Barnes, B., Kline, R. J., Vladar, A. E., Obeng, Y. S., and Davydov, A., "International Roadmap for Devices and Systems™ 2023 Edition Metrology," (2023).

[2] Zhu, J., Liu, J., Xu, T., Yuan, S., Zhang, Z., Jiang, H., Gu, H., Zhou, R., and Liu, S., "Optical wafer defect inspection at the 10 nm technology node and beyond," *International Journal of Extreme Manufacturing* **4**(3), 032001 (2022).

[3] Frase, C. G., Buhr, E., and Dirscherl, K., "CD characterization of nanostructures in SEM metrology," *Measurement Science and Technology* **18**(2), 510 (2007).

[4] Hussain, D., Ahmad, K., Song, J., and Xie, H., "Advances in the atomic force microscopy for critical dimension metrology," *Measurement Science and Technology* **28**(1), 012001 (2016).

[5] Silver, R. M., Barnes, B. M., Sohn, Y., Quintanilha, R., Zhou, H., Deeb, C., Johnson, M., Goodwin, M., and Patel, D., "The limits and extensibility of optical patterned defect inspection," in [*Metrology, Inspection, and Process Control for Microlithography XXIV*], **7638**, 182–194, SPIE (2010).

[6] Yoshioka, T., Miyoshi, T., and Takaya, Y., "Particle detection for patterned wafers of 100nm design rule by evanescent light illumination: analysis of evanescent light scattering using finite-difference time-domain (FDTD) method," in [*Optomechatronic Sensors and Instrumentation*], **6049**, 73–81, SPIE (2005).

[7] Kolenov, D., Zadeh, I. E., Horsten, R. C., and Pereira, S. F., "Direct detection of polystyrene equivalent nanoparticles with a diameter of 21 nm ($\lambda/19$) using coherent fourier scatterometry," *Optics Express* **29**(11), 16487–16505 (2021).

[8] Paul, A., Rafighdoost, J., Dou, X., and Pereira, S. F., "Investigation of coherent Fourier scatterometry as a calibration tool for determination of steep side wall angle and height of a nanostructure," *Measurement Science and Technology* **35**(7), 075202 (2024).

[9] Paul, A., Wever, R., Soman, S., and Pereira, S. F., "Utilizing focused field as a probe for shape determination of subwavelength structures via coherent Fourier scatterometry," *Physical Review Applied* **23**(2), 024016 (2025).

[10] Paul, A., Kolenov, D., Scholte, T., and Pereira, S. F., "Coherent Fourier scatterometry: a holistic tool for inspection of isolated particles or defects on gratings," *Applied Optics* **62**(29), 7589–7595 (2023).